

University of Denver

Digital Commons @ DU

Electronic Theses and Dissertations

Graduate Studies

2020

Microgrid-Enabled Reactive Power Support to Enhance Grid Economics

Sarhan Hasan

Follow this and additional works at: <https://digitalcommons.du.edu/etd>



Part of the [Computer Engineering Commons](#), and the [Power and Energy Commons](#)

MICROGRID-ENABLED REACTIVE POWER SUPPORT TO ENHANCE GRID
ECONOMICS

A Dissertation

Presented to

the Faculty of the Daniel Felix Ritchie School of Engineering and Computer Science

University of Denver

In Partial Fulfillment

of the Requirements for the Degree

Doctor of Philosophy

by

Sarhan Hasan

June 2020

Advisor: Dr. Amin Khodaei

©Copyright by Sarhan Hasan 2020

All Rights Reserved

Author: Sarhan Hasan
Title: MICROGRID-ENABLED REACTIVE POWER SUPPORT TO ENHANCE
GRID ECONOMICS
Advisor: Dr. Amin Khodaei
Degree Date: June 2020

Abstract

Reactive power plays an essential role in voltage control and stability in electric power systems. Various Volt/VAR techniques are utilized in electric power systems to maintain the voltage profile within defined acceptable limits and accordingly provide reliability and stability. Reactive power has been commonly generated through large-scale synchronous generators or distributed capacitor banks to provide proper transmission and distribution level system management, however, reactive power can be further used as an effective means to reduce total system operation cost. In this dissertation, an optimal reactive power model is proposed to determine the optimal nodal reactive powers that result in the lowest total system operation cost. Microgrid is introduced as a source of real and reactive power where its capability curve as a single generator unit is further determined and utilized. An optimization-based method is proposed to determine this capability curve. The results of numerical analyses of this proposal show how the reactive power behaves under gradual changing of real power generation in a microgrid and how these two outputs are correlated. This model is further integrated into an optimal power flow problem to show the potential economic benefits of microgrid-generated reactive power of the larger system. The numerical analyses on standard test systems show the performance of the proposed model and provide insights on the role of microgrid as a source of reactive power in the system.

Acknowledgment

First and foremost, I would like to express my sincere gratitude to my advisor, Dr. Amin Khodaei, for his valuable academic guidance, encouragement and continuous support throughout my research and study. I was privileged to be advised by him during my doctoral studies and I am forever grateful for his endless supports.

Besides my advisor, I would like to cordially thank my committee members, Dr. Kimon Valavanis, and Dr. Mohammad Matin for their time, feedbacks and support. My thanks also go to JB Holston, Dean of Ritchie School of Engineering and Computer Science, for his supports.

I deeply thank my family for their endless love, unconditional support and encouragement. They live in my home country, Libya, and I have not seen them for several years. Words cannot express how grateful I am to them for all of the sacrifices, supports and encouraging me with their best wishes.

I would also like to thank all my dear colleagues and friends at University of Denver and all friends in Denver.

TABLE OF CONTENTS

Preliminary Materials	
Abstract	ii
Nomenclature	vii
Chapter One: Introduction.....	1
Chapter Two: Reactive Power Support in Power system.....	10
2.1 Model outline and formulation of optimal Reactive power calculation.....	10
2.2 Numerical Simulation.....	12
2.2.1 Optimal Reactive Power at Large Scale Power system.....	12
2.2.2 Generators Capacity Changing Effect on the system operation cost.....	17
2.2.3 Optimal Reactive power at small scale Power System.....	21
3.2 Discussion.....	22
Chapter Three: Microgrid Capability Curve... ..	24
3.1. Capability Curve of Individual DERs	24
3.1.1. Synchronous Generator	25
3.1.2. Solar PV	25
3.1.3 Battery Energy Storage	26
3.2. Model Formulation	27
3.3. Numerical Simulation.....	28
3.4. Discussion.....	31
Chapter Four: Microgrid Effect on System Operation Cost	32
4.1. Model outline Formulation	32
4.2. Numerical Simulation.....	35
4.2.1 Microgrid Instillation at Critical bus	36
4.2.2 Microgrid Instillation at Noncritical bus	38
4.3 Discussion	41
Chapter Five: Conclusion and Future work	42
References.....	44
Appendix A: Matpower Codes	54
Appendix B: List of Publications	58

LIST OF FIGURES

Chapter Two.....	1
Figure 2.1: IEEE 57-bus standard system	13
Figure 2.2: Effect of optimum reactive power of buses on the system operation cost-for IEEE 57-bus system.....	16
Figure 2.3: Effect of generators' capacity decrease by 20 % on the objective function for 57-bus system.....	18
Figure 2.4: Effect of generators' capacity decrease by 40 % on the objective function for IEEE 57-bus.....	18
Figure 2.5: Effect of generators' capacity decrease by 60 % on the objective function for IEEE 57-bus	18
Figure 2.6: Effect of generators' capacity decrease by 80 % on the objective function for IEEE 57-bus.....	19
Figure 2.7: Effect of generators' capacity decrease by 100 % on the objective function for IEEE 57-bus.....	19
Figure 2.8: Effect of loads' real power decrease by 10 % on the system operation cost for IEEE 9-bus system	20
Figure 2.9: IEEE 9-bus system.....	20
Figure 2.10: Effect of optimum reactive power of buses on the objective function for IEEE 9-bus	20
Figure 2.11: IEEE 9-bus System	21
Figure 2.12: Effect of optimum reactive power on the system operation cost	22
Chapter Three.....	24
Figure 3.1: Synchronous Generator and solar PV capability curve.....	25
Figure 3.2: Battery energy storage	27
Figure 3.3: Capability curve of Microgrid for case 1.....	30
Figure 3.4: Capability curve of Microgrid for case 2.....	30
Figure 3.5: Capability curve of Microgrid for case 3.....	31
Chapter Four.....	32
Fig.4.1 Microgrid Capability Curve.....	33
Fig.4.2. IEEE Case57 – Bus System.....	36
Fig.4.3. Microgrid Effect on Object Function at Load Buses for Case IEEE case57.....	40

LIST OF TABLES

Chapter Two.....	1
Table 2.1. The Load Bus Data of Case IEEE 57.....	13
Table 2.2: Base vs Optimum Reactive Powers for P-Q Buses in IEEE 57-Bus System.....	15
Table 2.3: Total system operation cost for IEEE 9-bus and 57-bus system.....	17
Table 2.4: Critical Buses of Case IEEE 57.....	17
Table.2.5: Basic vs Optimal Reactive power for P-Q Buses in Case IEEE 9- Bus.....	22
Table 2.6: Basic case vs Unity Power Factor Objective Function for Case IEEE- 9.....	22
 Chapter Three	 24
Table 3.1: Microgrid DERs Capacities.....	29
 Chapter Four	 32
Table 4.1: Microgrid Characteristics of Generating units.....	37
Table 4.2. Total system Operation cost under basic reactive power	37
Table 4.3: Total system operation cost under different scenario –ignoring Micro grid capability curve for Case IEEE 57	37
Table 4.4: Microgrid Interconnected Sizes.....	39
Table 4.5: Total system operation cost under different scenarios – considering microgrid capability curve	39
Table 4.6: Total system operation cost under different scenarios – ignoring capability curve	39
Table 4.7: The system operation cost comparison between optimal reactive power and microgrid	41

NOMENCLATURE

Indices:

i	Index for units.
m, n	Index for buses.
t	Index for time.

Sets:

B	Set of buses.
G	Set of synchronous generators.
L	Set of lines.

Parameters:

a_p, b_p, c_p	Cost function coefficients.
b	Line susceptance.
g	Line conductance.
P^{\max}/Q^{\max}	Synchronous generator maximum real/reactive power.
PD/QD	Load real/reactive power.
PL^{\max}/QL^{\max}	Maximum real/reactive power flow of lines.
V^{\max}/V^{\min}	Maximum/minimum bus voltage magnitude.

Variables:

P/Q	Synchronous generator real and reactive power.
PL/QL	Line real/reactive power.
QM	Microgrid's reactive power to compensate bus's reactive power.
V	Bus voltage magnitude.
θ	Bus voltage angle.
p_g^{\min}	Lower active Power limit.
p_g^{\max}	Upper active power limit.
P_g	Generated Power.

CHAPTER ONE: INTRODUCTION

Reactive power plays a crucial role in power system stability and voltage control and is considered an essential ancillary service that supports the power system operation. Reactive power control can also potentially minimize system real power losses and accordingly reduce total system operation cost which is a less investigated problem. Various equipment can be found in power systems to manage reactive power, such as capacitors banks, flexible AC transmission system (FACTS) devices, and static voltage compensators (SVC) to name a few, further managed through various Volt/VAR control techniques [1-3]. The growing proliferation of distributed energy resources (DERs), however, introduces another viable source for reactive power generation which is primarily integrated to distribution grids.

The existing studies on reactive power mostly focus on its control, management and pricing [4-16]. A framework for reactive power management to protect voltage stability at maximum marginal value while keeping real and reactive power at a least-cost dispatch is presented in [4]. Reactive power shortage and the associated voltage violations due to the failures of reactive power sources are considered in [5], where reliability indices are proposed to represent the effect of reactive power shortage on system reliability. The control of real and reactive power exchange between inverter and utility grid using the d-q theory is proposed in [6]. A correction method is proposed in [7] to achieve rapid reactive power control on synchronous generators. A method to calculate the optimum real and

reactive power pricing that maximizes social benefit is presented in [8]. A comparison between the provision of reactive power support ancillary service in distribution systems and conventional equipment such as capacitor banks and distributed generation (DG) units based on renewable resources is provided in [9]. Design of a competitive market for reactive power ancillary services is discussed in [10], using a compromise programming approach based on a modified optimal power flow model. A mathematical model for reactive power pricing structure based on various cost components is developed in [11]. The study in [12] suggests a model to evaluate economical price of reactive power. The problem of reactive power ancillary services pricing is addressed and formulated as a joint cost allocation problem in [13]. A new multi-objective optimization method, based on reactive power clearing is proposed in [14], while considering system voltage stability. In [15], the authors investigate the possibility of designing a localized reactive power market. A competitive market for reactive power services in deregulated electricity systems, based on offers from reactive power resources, is presented in [16]. Existing literature investigates various methods of reactive power generation and control, with primary objectives of ensuring voltage stability and improved reliability. The cost optimization problem through reactive power control is however an important topic which needs further investigation and is lacking in the literature. In this dissertation, the optimal reactive power in all system nodes, which are capable of adjusting reactive power, is determined to minimize the system operation cost. A modified optimal power flow problem is defined and solved to find these optimum values, which is subject to all prevailing operational constraints. In addition, the model outline and formulation of the proposed optimum

reactive power calculation problem, and numerical simulations to show the performance of the proposed model on standard test systems are provided in chapter two.

A microgrid is a small scale power grid, operated at low voltage level, which is implemented by integrating various distributed energy resources (DERs) with the goal of improving local reliability, resilience, and power quality [17]-[19]. In addition to all merits of microgrids, microgrids have also been considered as viable ancillary service providers to utility grids and by increasing their penetration in the network, this role is now ever more attractive [20]-[22]. Considering that all common microgrid DERs can produce reactive power (diesel generators and microturbine through their synchronous generator and solar PV, wind, and batteries through their power electronics interface), microgrids can potentially provide reactive power support to the utility grid in terms of both injecting or withdrawing reactive power.

The reactive power management and voltage stability are strongly related to each other to keep voltage in its proper operational limits. Reactive power requirements usually change over time as loads change and accordingly inductors are used to manage high voltage on transmission systems, while capacitors are used to control low voltage on both transmission and distribution systems. In [23], an optimal reactive power dispatch is proposed to improve voltage stability margin and increase reactive power reserve. Droop control is introduced to adjust reactive power in order to keep voltage stability in microgrids [24, 25].

In order to provide the ancillary services to the utility grid, the amount of exchanged real and reactive power between microgrid and the utility grid should be managed. Therefore, obtaining the microgrid power exchange capability, both real and reactive

power, is important. The capability curve of DERs could be defined as a boundary within which the generator operates safely. Accordingly, reaching to microgrid capability curve is the first and most important step for microgrid owners in order to contribute to ancillary service needs of the grid. To this end, the capability curve of all DERs in microgrid should be combined to achieve an integrate capability curve for the microgrid.

In synchronous generators, the P-Q capability curve is ruled by some constrains that are explained and calculated in [26]. Leveraging solar PV as a reactive power source and determining its limits and capacity is described in [27]. The possibility of using solar PV as a source of ancillary services to support reactive power compensation, as well as modeling an approach to develop capability curve of solar PV using an advanced control method is proposed in [28]. Real and reactive power in solar PVs could be controlled by various algorithms, applicable to fixed real power mode and maximum power point tracking (MPPT) control mode, that provide fast reactive power with voltage stability during switching between these two modes as discussed in [29]. Energy storage systems could also be used to improve the power quality, including frequency and voltage level and support the system with needed backup power [30]. The battery energy storage system would help in mitigating power fluctuations of PV units and wind turbines under various weather conditions [31]. During the daytime, the battery gets charged from PV system, and during the nighttime the battery discharges to the critical loads or feeds the grid for reactive power and harmonic compensations. A reactive power controller is designed in [32] to control the amount of reactive power delivered to the grid. This controller operates based on power factor measurement.

In this study, the real-reactive power capability curve of a microgrid with various DERs is determined. To achieve such a curve, the reactive power profile at different load points is determined using a proposed optimization-based method, and consequently the capability curve is drawn. By obtaining capability curve of the microgrid, the microgrid with different DERs is seen as a single unit in the network, or a virtual power plant, with the ability to offer reactive power. Furthermore, the limits of reactive power for each individual DER, and the capability curve of a microgrid is calculated using the proposed optimization-based method and explained in chapter three.

It has become a growing trend to deploy microgrids in critical points of the grid so that in the event of failure of the main grid, the microgrid is able to maintain the continuity of supply and meeting constraints of security, reliability, and supply quality. A microgrid connects to the grid at a point of common coupling that follows the same voltage and frequency as the main. A microgrid not only provides backup for the grid in case of emergencies, but can also be used to reduce operation costs, or connect to a local resource that is too small or unreliable for traditional grid use. A microgrid allows communities to be more energy independent and, in some cases, more environmentally friendly.

Reactive power has always been an indispensable part of a reliable and stable grid operation, both at generation and delivery sides. However its importance is increasing as the demand for electric power grows and the type of loads, which are more inductive in many cases, changes. Traditionally, equipment such as capacitor banks, inductive reactors, and flexible AC transmission system are used to manage reactive power. A detailed discussion on primary sources of reactive power is provided in [33].

Ancillary services support power delivery from generation site all the way to the customers. Ancillary services include load regulation, spinning reserve, non-spinning reserve, replacement reserve, and voltage support. Reactive power, as a primary source of voltage support, has a profound effect on real power transfers and on security of power system as it affects the voltage profile throughout the system, makes the power system more reliable, and guarantees feasible power flow. However reactive power cannot be transported over large distances [34].

There has been extensive research on the generation and delivery of reactive power. Reactive power control and distribution face many challenges specifically in the presence of wind and photovoltaic sources. A correction method is proposed in [35] to achieve rapid reactive power control on synchronous generators. Reactive power shortage and the associated voltage violations due to the failures of reactive power sources are considered in [36]. A control strategy for reactive power compensation is presented in [37]. A methodology to represent the reactive power generation limits in the power flow problem is proposed in [38] by using a set of sigmoid switches that incorporate new equations into the problem formulation. Three models are presented in [39] to solve the optimal reactive power flow in a wind generation integrated power system. The overview of the possibilities, limits, pros and cons of the reactive power control of wind turbines are explained in [40]. The description of the developed methods of definition of a payment for voltage and reactive power control by power stations is discussed in [41]. The control of active and reactive power between inverter and utility grid using the d-q theory has been proposed in [42]. The interfacing and interconnection of DG units in microgrid to general grid is offered usually by power electronic devices to provide control. However, there are

power quality problems caused by these devices, and reactive power compensation represents one of them in supporting load and voltage. Reactive power/voltage and real power/frequency are discussed as main tools in controlling power in microgrids [43]. The reactive power droop control was presented in [44] where voltage reduction is done by integration of the reactive power. In this control method, microgrids operate as active power filter to get harmonic compensation of reactive power. All these control techniques are applied in microgrids to achieve reactive power compensation.

The study in [45] suggests a model to evaluate economical price of reactive power. Authors in [46] propose reactive power pricing to incorporate the operation cost of generators for the reactive power production cost as an ancillary service. Authors in [47] present a methodology to remunerate the ancillary services of generation reserve and reactive power support as a function of the benefit provided by generators to the power system. A method of equivalent reactive power compensation is proposed to measure the difference among reactive power resource value in [48]. In [49], particle swarm optimization and its variants are applied to calculate the optimal real and reactive power to manage power congestion in the system. A framework for reactive power management to protect voltage stability at maximum marginal while keeping active and reactive power at economical dispatch is presented in [50]. A detailed model is presented for the incorporation of the distributed generation (DG) units' reactive power limits in the power flow formulation in [51]. Reactive power shortage and the associated voltage violations due to the failures of reactive power sources are considered in [52] where new reliability indices are proposed to represent the effect of reactive power shortage on system reliability. A model to find optimum real and reactive power in embedded wind generation and battery

energy storage system is proposed in [53]. A novel solution for optimal reactive power dispatch problem is handled by a new mathematical approach for voltage magnitudes in [54]. Reactive power cost is divided into reactive power capacity cost and reactive electricity quantity cost in [55]. Studies in [56] suggest that maximum profit of reactive power can be obtained when the marginal revenue equals marginal cost.

The problem of pricing reactive power ancillary services is addressed and formulated as a joint cost allocation problem in [57]. The investigation of the extent of forecasting electricity prices of ancillary services over a 24-hour horizon is illustrated in [58]. A method to calculate the optimum real and reactive power that maximizes social benefit and minimizes the operation cost of power system is presented in [59]. A mathematical model for reactive power pricing structure based on various cost components is developed in [60]. The design of a competitive market for reactive power ancillary services is discussed in [61] using a compromise programming approach based on a modified optimal power flow model. A reactive power economic dispatch method is proposed using power flow simulator in [62]. In [63], reactive power cost is analyzed using theory of marginal cost at various loads. It is discussed in this study that power factor penalty of load and addition of reactive power cost to real power cost are two methods to recover reactive power cost.

Moreover, it is discussed that reactive power generation leads to a reduction in real power generation. As a result, an opportunity cost of reactive power is introduced to recover real power production. Moreover, capacitive reactive power cost and its allocation are evaluated to get minimum cost using linear programming techniques. Reactive power could be provided by renewable sources to distribution grids which would reduce the

transmission system operation cost, improve system security, and reduce ancillary services cost [64].

In this dissertation, the microgrid is introduced as a source of reactive power to determine its effect on system operation cost. The difference between the optimal reactive power and the original reactive power is calculated and supplied by installing microgrids in proper buses. It is shown that the unity power factor at all buses does not necessarily minimize power losses and generation cost, but the combination of positive and negative reactive powers at various buses in the system would minimize the operation cost. The model outline and formulation of optimum reactive power is calculated in chapter four for power system including microgrid operation at critical and noncritical buses with numerical simulation.

The main contributions of this dissertation are listed as follows:

- The optimum reactive power at conventional power system that ensures minimum system operation cost is determined at each load (P-Q) bus.
- Critical buses where the system operation cost is most minimized are determined.
- A capability curve of the microgrid as one aggregate unit instead of individual DERs is determined.
- A microgrid as a source of real and reactive power is introduced to the system to measure its impact on the system operation cost.

CHAPTER TWO: REACTIVE POWER SUPPORT IN POWER SYSTEM

1.1 Model Outline And Formulation Of Optimum Reactive Power Calculation

The goal of the proposed model is to determine the optimal nodal reactive powers that guarantee a minimum total system operation cost. In other words, the nodal reactive powers are adjusted in a way that the cost of real power generation in the system is minimized. The system operation cost is defined in (2.1) as the sum of individual unit costs, each presented as a second order function of its real power generation. P_i represents real power generation of unit i and a , b , and c represent constant cost coefficients. This objective is subject to operational constraints (2.2)-(2.10).

$$\min \sum_i (a_i P_i^2 + b_i P_i + c_i) \quad (2.1)$$

$$P_i^{\min} \leq P_i \leq P_i^{\max} \quad \forall i \in G \quad (2.2)$$

$$Q_i^{\min} \leq Q_i \leq Q_i^{\max} \quad \forall i \in G \quad (2.3)$$

$$PL_{mn} = g_{mn} V_m^2 - V_m V_n (g_{mn} \cos(\theta_m - \theta_n)) - V_m V_n (b_{mn} \sin(\theta_m - \theta_n)) \quad \forall mn \in L \quad (2.4)$$

$$QL_{mn} = -b_{mn} V_m^2 - V_m V_n (b_{mn} \cos(\theta_m - \theta_n)) - V_m V_n (g_{mn} \sin(\theta_m - \theta_n)) \quad \forall mn \in L \quad (2.5)$$

$$-PL_{mn}^{\max} \leq PL_{mn} \leq PL_{mn}^{\max} \quad \forall mn \in L \quad (2.6)$$

$$-QL_{mn}^{\max} \leq QL_{mn} \leq QL_{mn}^{\max} \quad \forall mn \in L \quad (2.7)$$

$$\sum_{i \in G_m} P_i + \sum_{n \in B_m} PL_{mn} = PD_m \quad \forall m \in B \quad (2.8)$$

$$\sum_{i \in G_m} Q_i + \sum_{n \in B_m} QL_{mn} = QD_m + QM_m \quad \forall m \in B \quad (2.9)$$

$$V_m^{\min} \leq V_m \leq V_m^{\max} \quad \forall m \in B \quad (2.10)$$

$$QM_m^{\min} \leq QM_m \leq QM_m^{\max} \quad \forall m \in B \quad (2.11)$$

The limits of real power (P) and reactive power (Q) of synchronous generation unit (i) are shown in (2.2)-(2.3). G represents the set of all generation units. Equations (2.2) and (2.3) can be further linked and extended using each unit's capability curve. Synchronous generator's capability curves are provided by manufacturers and used for loading the synchronous generators in different operating loads without exceeding the designed limits. Generally, nominal capacity of a synchronous machine can be indicated by MVA in a specific voltage and power factor (usually 85-90% leading) in which the synchronous machine is able to work continuously without abnormal temperature increment. Real power output of the synchronous machine depends on turbine ability and nominal MVA machine limits. The maximum reactive power capability is associated with operating with lagging power factor and the minimum reactive power capability corresponds to the maximum reactive power the generator may absorb when operating with leading power factor. Lines' real power flow (PL) and reactive power flow (QL) equations are presented in (2.4) and (2.5), respectively, based on nodal voltage magnitudes (V), voltage angles (θ), and lines conductance (g) and susceptance (b). m and n are indices for system buses and L is the set of transmission lines. Equations (2.6) and (2.7) ensure that lines' real and reactive power flows are limited to their respective capacities. The nodal real and reactive power balance equations (2.8)-(2.9) ensure that the sum of nodal real and reactive power injections from generators and the power injected/withdrawn through the lines connected to each node, equals the real load (PD) and reactive load (QD) at that bus. G_m and B_m respectively represent the set of generation units and lines connected to bus m . Nodal voltage magnitudes are also restricted by their respective limits as in (2.10).

To consider the role of DERs in reactive power generation/consumption, a new variables (QM) is defined and added to the reactive power balance equation. This variable represents the amount of reactive power that DERs contribute to each node, and is restricted by its respective limits as in (11). These limits are determined based on the capability curve and the amount of real power that DERs are producing. It should be noted that in (2.9) the impact of DERs (connected to the distribution network) is considered in the transmission network, so the employed variable is an aggregate number for all the DERs connected to that specific transmission bus. As this is a free variable in the optimal power flow problem and merely bound by its limits, it will reach an optimal value that minimizes the system operation cost.

2.2 Numerical Simulation

The proposed model is formulated in MATPOWER and applied to two standard IEEE test systems. The IEEE 57-bus standard test system, as a relatively large-scale system, is shown in Fig. 2.1. This system consists of seven generators and fifty P-Q buses. The IEEE 9-bus system represents the small-scale system with three generators and six P-Q buses.

1.2.1 Optimal Reactive Power at Large Scale Power system

The IEEE 57-bus standard test system represents large scale system as shown in Fig. 2.1. This system consists of seven generators and fifty PQ buses with data as shown in Table 2.1.

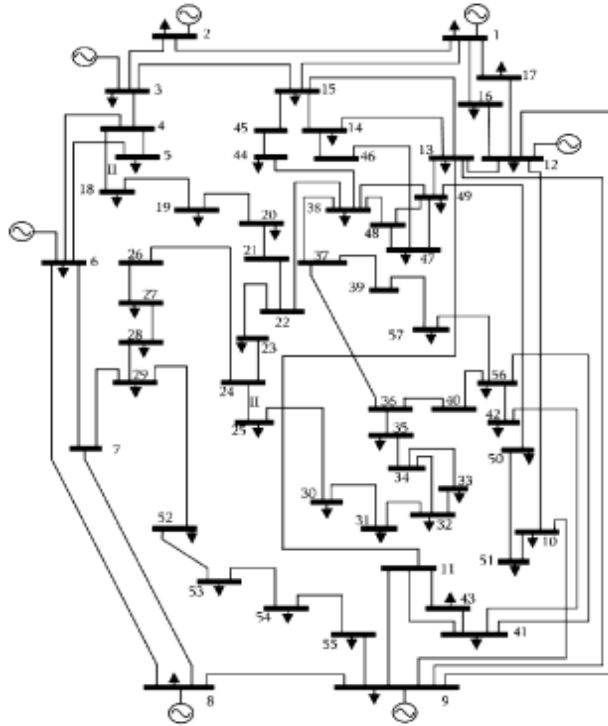


Figure 2.1. IEEE 57-bus standard system.

Table.2.1. The Load Bus Data of Case IEEE 57

Bus	Type	P_d	Q_d	G_s	B_s	Area	V_m	V_a	V_{max}	V_{min}
1	3	55	17	0	0	1	1.04	0	1.06	0.94
2	2	3	88	0	0	1	1.01	-1.18	1.06	0.94
3	2	41	21	0	0	1	0.985	-5.97	1.06	0.94
4	1	0	0	0	0	1	0.981	-7.32	1.06	0.94
5	1	13	4	0	0	1	0.976	-8.52	1.06	0.94
6	2	75	2	0	0	1	0.98	-8.65	1.06	0.94
7	1	0	0	0	0	1	0.984	-7.58	1.06	0.94
8	2	150	22	0	0	1	1.005	-4.45	1.06	0.94
9	2	121	26	0	0	1	0.98	-9.56	1.06	0.94
11	1	0	0	0	0	1	0.974	-10.1	1.06	0.94
12	2	377	24	0	0	1	1.015	-10.46	1.06	0.94;
13	1	18	2.3	0	0	1	0.979	-9.79	1.06	0.94;
14	1	10.5	5.3	0	0	1	0.97	-9.33	1.06	0.94
15	1	22	5	0	0	1	0.988	-7.18	1.06	0.94
16	1	43	3	0	0	1	1.013	-8.85	1.06	0.94;
17	1	42	8	0	0	1	1.017	-5.39	1.06	0.94;
18	1	27.2	9.8	0	10	1	1.001	-11.71	1.06	0.94;

19	1	3.3	0.6	0	0	1	0.97	-13.2	1.06	0.94
20	1	2.3	1	0	0	1	0.964	-13.41	1.06	0.94
21	1	0	0	0	0	1	1.008	-12.89	1.06	0.94
22	1	0	0	0	0	1	1.01	-12.84	1.06	0.94
23	1	6.3	2.1	0	0	1	1.008	-12.91	1.06	0.94
24	1	0	0	0	0	1	0.999	-13.25	1.06	0.94
25	1	6.3	3.2	0	5.9	1	0.982	-18.13	1.06	0.94
26	1	0	0	0	0	1	0.959	-12.95	1.06	0.94
27	1	9.3	0.5	0	0	1	0.982	-11.48	1.06	0.94
28	1	4.6	2.3	0	0	1	0.997	-10.45	1.06	0.94
29	1	17	2.6	0	0	1	1.01	-9.75	1.06	0.94
30	1	3.6	1.8	0	0	1	0.962	-18.68	1.06	0.94
31	1	5.8	2.9	0	0	1	0.936	-19.34	1.06	0.94
32	1	1.6	0.8	0	0	1	0.949	-18.46	1.06	0.94
33	1	3.8	1.9	0	0	1	0.947	-18.5	1.06	0.94
34	1	0	0	0	0	1	0.959	-14.1	1.06	0.94
35	1	6	3	0	0	1	0.966	-13.86	1.06	0.94
36	1	0	0	0	0	1	0.976	-13.59	1.06	0.94
37	1	0	0	0	0	1	0.985	-13.41	1.06	0.94
38	1	14	7	0	0	1	1.013	-12.71	1.06	0.94
39	1	0	0	0	0	1	0.983	-13.46	1.06	0.94
40	1	0	0	0	0	1	0.973	-13.62	1.06	0.94
41	1	6.3	3	0	0	1	0.996	-14.05	1.06	0.94
42	1	7.1	4.4	0	0	1	0.966	-15.5	1.06	0.94;
43	1	2	1	0	0	1	1.01	-11.33	1.06	0.94
44	1	12	1.8	0	0	1	1.017	-11.86	1.06	0.94
45	1	0	0	0	0	1	1.036	-9.25	1.06	0.94
46	1	0	0	0	0	1	1.05	-11.89	1.06	0.94
47	1	29.7	11.6	0	0	1	1.033	-12.49	1.06	0.94
48	1	0	0	0	0	1	1.027	-12.59	1.06	0.94
49	1	18	8.5	0	0	1	1.036	-12.92	1.06	0.94

50	1	21	10.5	0	0	1	1.023	-13.39	1.06	0.94
51	1	18	5.3	0	0	1	1.052	-12.52	1.06	0.94
52	1	4.9	2.2	0	0	1	0.98	-11.47	1.06	0.94
53	1	20	10	0	6.3	1	0.971	-12.23	1.06	0.94
54	1	4.1	1.4	0	0	1	0.996	-11.69	1.06	0.94
55	1	6.8	3.4	0	0	1	1.031	-10.78	1.06	0.94
56	1	7.6	2.2	0	0	1	0.968	-16.04	1.06	0.94
57	1	6.7	2	0	0	1	0.965	-16.56	1.06	57

The reactive power is initially considered to be fixed and equal to the values provided by the input data. The operation cost in this case is calculated as \$41738. To minimize the total operation cost, the reactive power at each bus, individually, is considered to be variable (i.e., a reactive power source is available at that bus) and the optimal reactive power is calculated accordingly. The results of the optimal reactive power in each bus are listed in Table 2.2, and the corresponding costs are shown in Fig. 2.2 As the results demonstrate, some buses have a large effect on the system operation cost, while others have a relatively smaller effect, showing the criticality of some buses over others in impacting the system operation cost.

As shown in Table.2.4, buses 35, 36, and 40 share the highest effect on the total system operation cost. These results suggest that it would be logical to focus only on a handful of buses in the system for reactive power generation, as these buses may have a larger impact than the sum of many other buses.

Table 2.2. Base vs Optimum Reactive Powers for P-Q Buses in IEEE 57-Bus System

Load bus number	Basic reactive power (MVAR)	Optimum reactive power (MVAR)
4	0	1.77

5	4	2.47
7	0	55.21
16	3	1.13
18	9.8	-5.58
21	0	-4.41
23	2.1	-0.46
25	3.2	0.85
27	0.5	177
29	2.6	-49.34
31	2.90	3.00
33	1.90	1.90
36	0	0.08
40	0	40
42	4.4	4.82
51	5.3	-78.26
52	2.2	-1.68
54	1.4	1.66
57	2	0.27

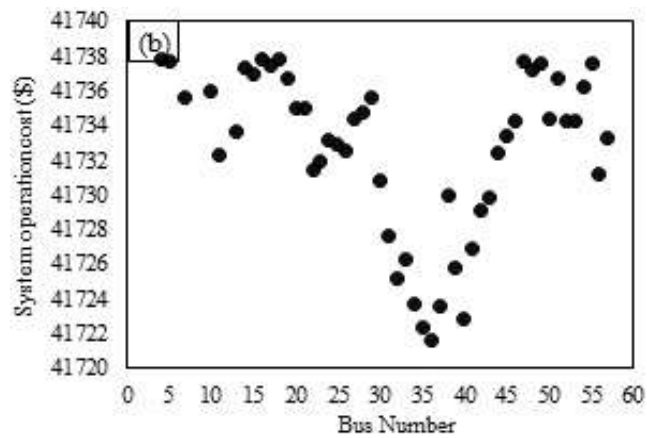


Figure 2.2. Effect of optimum reactive power of buses on the system operation cost- for IEEE 57-bus system.

Table.2.3 shows a comparison of total system operation cost for the base case, considering unity power factor for all buses (associated with $Q=0$), and after finding optimum reactive power. The results indicate that having unity power factor at all buses

does not necessarily lead to the minimum system operation cost. A comparison of the costs show that a unity power factor in all buses reduces the cost by around 0.03% while this reduction for the optimum reactive power case is 0.04%. This may seem as a small percentage, however considering the extremely large operation cost of practical systems (in range of millions of dollars daily), this reduction can lead to significant savings.

Table 2.3. Total system operation cost of 57-bus systems

Test system	Base case (without applying optimization)	Q=0 in all load buses (unity power factor)	After applying optimization
IEEE 57-Bus System	\$41738	\$41724	\$41721.7

Table 2.4. Critical Buses of Case IEEE 57

Critical Load Bus Number	System Operation Cost \$/h	Decreasing Percent
36	41721.65	-0.038
35	41722.27	-0.037
40	41722.84	-0.035
37	41723.59	-0.034
34	41723.68	-0.033
32	41725.21	-0.030
39	41725.71	-0.028
33	41726.28	-0.027
41	41726.87	-0.026
31	41727.61	-0.024
42	41729.12	-0.020
43	41729.79	-0.019

2.2.2 Generators Capacity Changing Effect on the system operation Cost

In this case, the generators' capacity is changed one by one. First, the capacities are decreased by steps of 20% and the results are shown in Figs.2.3 - 2.7. As shown in the

figures, by decreasing capacities, the system operation cost increases because when a generator's capacity decreases below its original operating point, the generator would not be able to fully supply the loads. Therefore, the loads supplied by that generator should be supplied by other generators which are farther. As a result, the system losses are increased and the total generation cost increases too. By increasing generators' capacities, the system operation cost does not change as the operating point of each generator would not change.

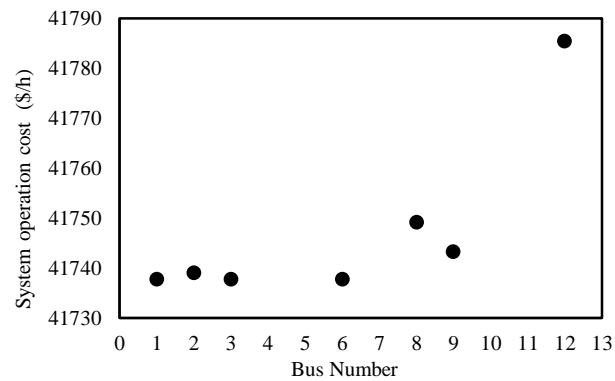


Fig. 2.3. Effect of generators' capacity decrease by 20 % on the objective function for IEEE 57-bus system

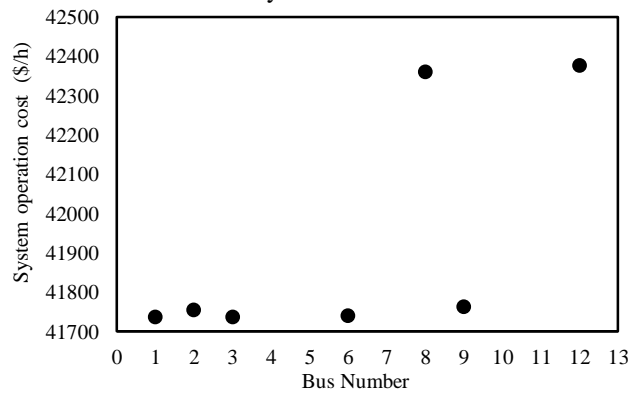


Fig 2.4. Effect of generators' capacity decrease by 40 % on the system operation cost for IEEE 57-bus system

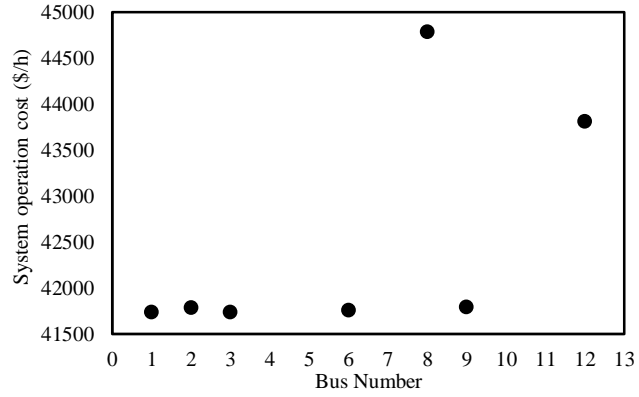


Fig.2.5. Effect of generators' capacity decrease by 60 % on the system operation cost for IEEE 57-bus system

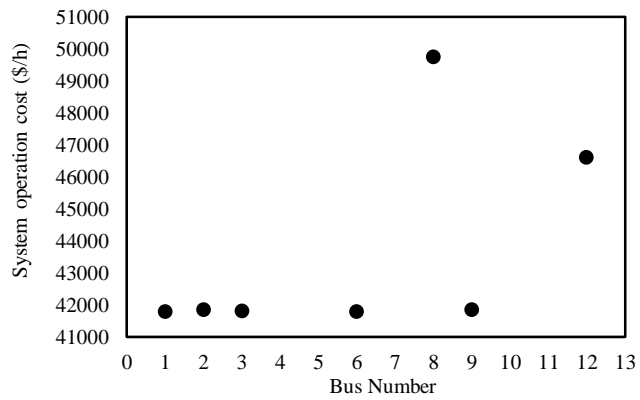


Fig.2.6. Effect of generators' capacity decrease by 80 % on system operation cost for IEEE 57-bus system

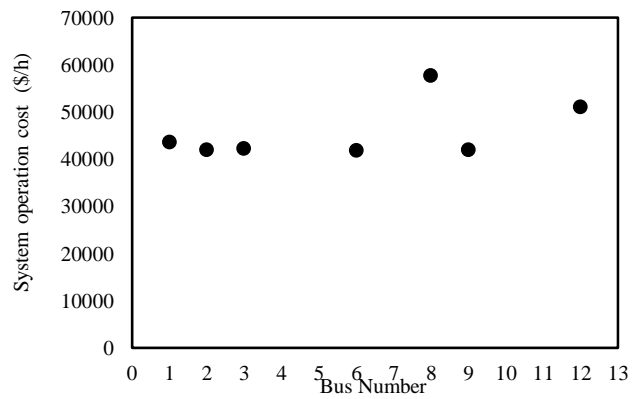


Fig.2.7. Effect of generators' capacity decrease by 100 % on the system operation cost for IEEE 57-bus system

In other this case, the real power of loads in all P-Q buses is changed one by one by the steps of 10%. The results are shown in Fig.4.8 - 4.10. As shown in the figures, by decreasing loads, the system operation cost decreases because less power is required to be generated by generators and hence the operation cost would decrease. The system operation cost in some buses, such as buses 16 and 17, is associated with a smaller number. It means that these buses are critical and by having optimum reactive power at these buses, the generation cost would decrease significantly.

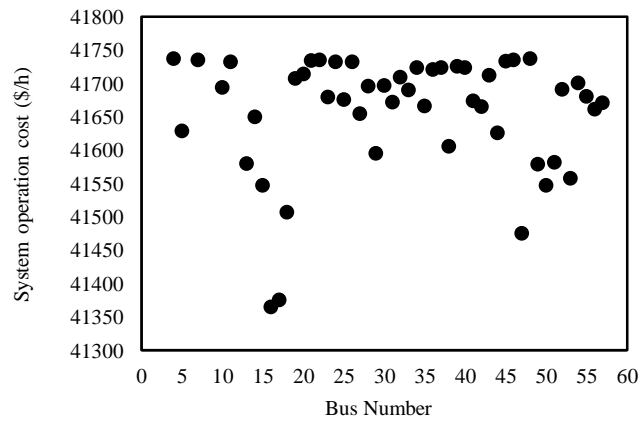


Fig.2.8 Effect of loads' real power decrease by 10 % on system operation cost

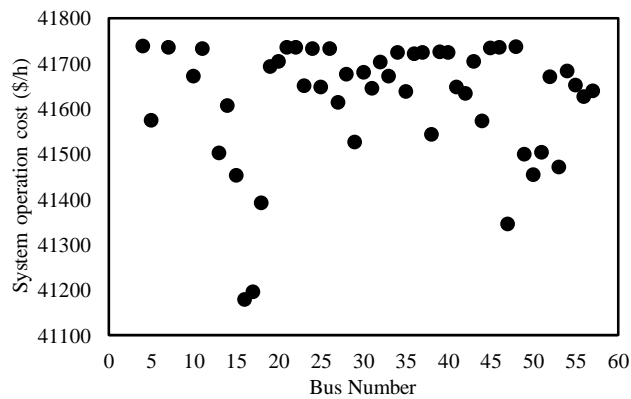


Fig.2.9 Effect of loads' real power decrease by 20 % on system operation cost

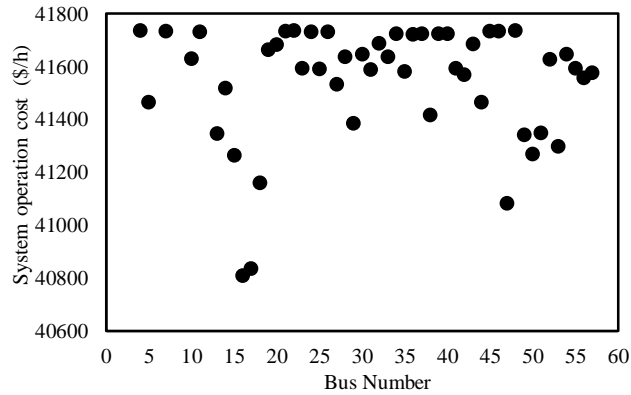


Fig.2.10 Effect of loads' real power decrease by 40 % on system operation cost

2.2.3 Optimal Reactive power at small scale Power System

The IEEE 9-bus system represents a small-scale power system with three generators and six P-Q buses as illustrated in Fig.2.11. During algorithm execution, if the optimum reactive power of any bus is at any of its limits, the reactive power constraint should be increased, and the code should be run again to calculate the new optimum reactive power at that bus. The reactive power before and after applying optimization model is calculated for IEEE 9-bus. Table.2.5 illustrates both the basic and optimum reactive power results for a few buses. During code execution for both cases, all reactive powers are changed to zero before optimum calculation. Fig.2.10 shows how the system operation cost changes by having the optimum reactive power at each bus in IEEE 9-bus system. Some buses have a large effect on the basic system operation cost, while others have a small effect on that. As shown in Fig.2.11, bus 9 has the highest effect on the system operation cost with the value of \$5295/h, while buses 6 and 8 represent the lowest impact. Therefore, modifying a power system to find optimum reactive power in certain P-Q buses instead of all buses would save money and reduce the number of equipment needed for reactive power compensation such as capacitor banks.

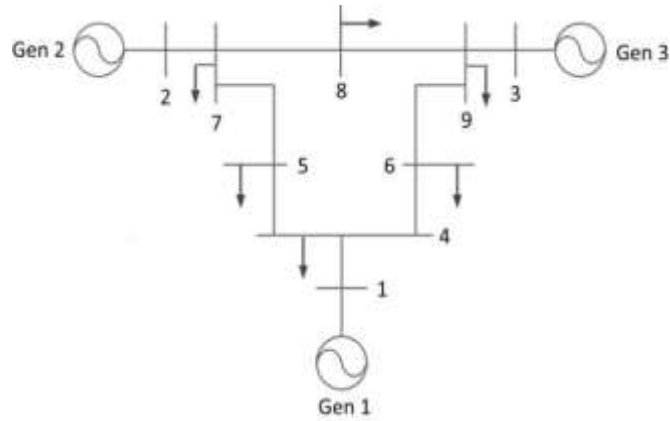


Fig.2.11. IEEE 9-bus system

Table.2.5 Basic vs Optimal Reactive Power for P-Q buses in Case IEEE 9

Load Bus Number	Basic Reactive Power (MVAR)	Optimum Reactive Power (MVAR)
4	0	53.01
5	30	-25.50
6	0	55.27
7	35	-17.98
8	0	60.73
9	50	-20.15

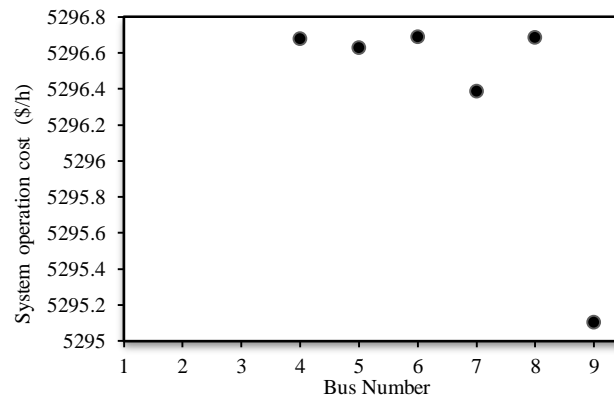


Fig.2.12 Effect of optimum reactive power of buses on the system operation cost for IEEE 9 -bus system.

Table 2.6 Results of Basic, Unity power factor, and Optimization

System	Basic Result without Applying Optimization	Objective function when $Q=0$ for all load buses (unity power factor)	Minimum objective function after applying optimization
IEEE 9-BUS SYSTEM	5296.7	5297.8	5295.1

2.3 Discussion

Reactive power has a crucial role in voltage control, and accordingly reliability and stability of power systems. In addition, reactive power is an important factor in reducing system losses. One of main purposes of this study was to find optimum nodal reactive power in a power system such that the total system operation cost is minimized. To this end, a nodal reactive power variable was added to the optimal power flow problem, and the critical buses which showed the highest effect on decreasing the system operation cost were determined. The required reactive power adjustments were considered to be supplied by DERs and microgrids. The proposed model was tested on the IEEE 57-bus system as a large scale power system and on IEEE 9-bus system as a small scale power system, and the obtained results showed that the unity power factor at all buses does not necessarily minimize system operation cost, but the combination of positive and negative reactive powers at various buses in the system would help achieve this objective.

CHAPTER THREE: MICROGRID CAPABILITY CURVE

The capability curve of generators is essential in power system operation as it determines a generator's capability in delivering real and reactive powers. Reactive power dispatch is an integral part of power system operation to ensure system load balance and further manage voltage stability. Although these capability curves are provided by generator's manufacturers and readily available for power system studies, the same is not true for microgrids which comprise various distributed energy resources. The main purpose of this study is to find the capability curve of a microgrid as a single unit (i.e., a virtual power plant) in a distribution grid. Obtaining the capability curve of the microgrid provides the microgrid owner with a better understanding on how much ancillary services the microgrid can offer to the utility grid, mainly via reactive power production. To determine the microgrid capability curve, an optimization-based method that identifies the maximum and minimum reactive power capability in various real power operation points is proposed.

3.1 Capability Curve Of Individual DERS

The capability curve of any electrical generator determines a region where can the generator works stable, and the operation point of the generator should be inside the capability curve. The capability curve of a microgrid is determined based on the individual capability curve of each of its DERS. The discussion on the capability curve of synchronous generator, solar PV, and battery energy storage is provided below.

3.1.1 Synchronous Generator

Synchronous generators are the most common technology for power generation, used in thermal, hydro and nuclear units. The capability curve of a synchronous generator is commonly considered as a semicircle with radius S as apparent power, as shown in Fig.3.1, where there could exist additional limiting factors that affect its circular shape. The relation between real power (P) and reactive power (Q) is shown in (3.1) and the limits of apparent (S), real, and reactive powers are illustrated in (3.2)-(3.4), respectively.

$$S^2 = P^2 + Q^2 \quad (3.1)$$

$$0 \leq S \leq S^{max} \quad (3.2)$$

$$0 \leq P \leq P^{max} \quad (3.3)$$

$$Q^{min} \leq Q \leq Q^{max} \quad (3.4)$$

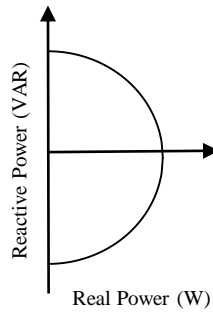


Figure 3.1. Synchronous Generator and Solar PV capability curve.

3.1.2 Solar PV

The PV unit contains three elements: PV panel array, inverter, and transformer [65]. The PV unit is controlled to operate at MPPT and the PV array is modeled as a current source connected in parallel with a capacitor, while the inverter is modeled as a voltage source. The PV unit's output power depends on weather conditions and solar radiation

during the day. Maximum delivered real power by PV unit occurs at maximum solar radiation and minimum temperature [66]. The DC voltage of solar PV inverters may limit the reactive power capability of the inverters. The reactive power capability of clustered inverters in PV units is analyzed in [67]. The relationships between apparent, real, and reactive powers are as those in (3.1)-(3.4) for a solar PV unit, and the capability curve is shown in Fig (3.1), the same as for a synchronous generator.

3.1.3 Battery Energy Storage

The battery energy storage is used to seamlessly supply the loads during peak hours and to capture power fluctuations of variable DERs. The battery energy storage system has two operating modes of charging and discharging, in which its power is positive at discharging mode and negative at charging mode. The battery energy storage system's capability curve that relates real power and reactive power is a circle with radius S , and with both leading and lagging power factors associated with its operating modes, as shown in Fig 3. 2. The relation between real power (P) and reactive power (Q) of battery energy storage system is shown in (3.5) and the limits of apparent power (S), real power (P), and reactive power (Q) are illustrated in (3.6)-(3.9), respectively.

$$S^2 = P^2 + Q^2 \quad (3.5)$$

$$S^{min} \leq S \leq S^{max} \quad (3.6)$$

$$P^{min} \leq P \leq P^{max} \quad (3.7)$$

$$Q^{min} \leq Q \leq Q^{max} \quad (3.8)$$

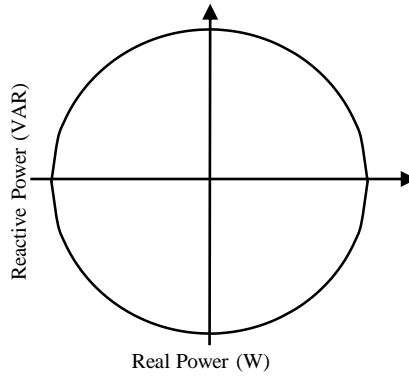


Figure 3.2. Battery energy storage capability curve.

3.2 Model Formulation

To find the microgrid capability curve, an optimization model is proposed as follows:

$$\min/\max Q \quad (3.9)$$

s. t.

$$P_s + P_b + P_g = P_d \quad (3.10)$$

$$\text{and (3.1) – (3.8)} \quad (3.11)$$

The objective of this model is to find the minimum and the maximum reactive power that can be produced by the microgrid (3.9) based on the net real power it produces. This objective is subject to a load balance constraint (3.10) in which the summation of power output of solar PV (P_s), battery (P_b) and the synchronous generator (P_g) equals a hypothetical net load (P_d). The objective is further subject to constraints associated with individual DERs' capability curves as in (3.11). Variables P_s and P_g are positive, while P_b can be either positive or negative based on the battery's charging and discharging state. P_d is initially assumed to be equal to the maximum charging power of the battery (a negative value) and then in each several iterations P_d is increased by a selected step. In each iteration for the selected P_d value, minimum and maximum amount of reactive power that can be

produced (two points) are calculated and then P_d is increased by the selected step. This process continues until P_d reaches the generation capacity of the microgrid. In that point the reactive power generation will reach zero as all DERs will generate maximum real power and therefore their respective reactive power generations will be zero, i.e., intersection of their capability curves with the horizontal real power axis.

Given the small size of this optimization problem, a very small step can be considered and the problem can be solved from several iterations to find a very accurate capability curve. The proposed model is generic and can consider any number of DERs as long as individual capability curves are available.

3.3 Numerical Analyses

A microgrid consisting of a small scale synchronous generator, a solar PV, and an energy storage is considered. The output of all of those generators are interconnected in parallel to work as one plant. In order to cover various conditions of the microgrid capability curve, three cases with various power capacities for microgrid DERs are considered as follows:

Case 1: All three DERs have the same capacity.

Case 2: Two DERs (PV and energy storage) have the same capacity while the synchronous generator is larger.

Case 3: The DERs have different capacities.

The capacities of microgrid components in aforementioned cases are tabulated in Table 3.1.

Table 3.1 Microgrid DERs Capacities

Case Number	Synchronous generator (MVA)	Solar Photovoltaic (MVA)	Energy Storage (MVA)
Case 1	10	10	10
Case 2	20	10	10
Case 3	15	5	10

The proposed model is applied to these cases and the obtained results are plotted in Figs. 3-5. As the figures show, capability curve of microgrid in all three cases are different from capability curve of each component of the microgrid, i.e. semicircle for synchronous generator and solar PV, and full circle for energy storage. Moreover, the figures clearly prove that the capability curve of the microgrid depends on the capacities of its DERs.

Capability curve of microgrid in all three cases are non-symmetrical, however, Case 1 Fig.3.3 has the closest curve to capability curve of each DER since the capacity of all components are the same. Capability curve of microgrid in Case 2 Fig 3.4 has a breakpoint, stemming from the different capacity of the synchronous generator. Fig. 3.5 depicts the most non-symmetrical figure, belonging to Case 3, with two breakpoints in the curve which stems from the difference in capacities. Thus, the results demonstrate that the shape of microgrid capability curve is affected by the size of units in the microgrid for each case.

It is interesting to note that the shape of the microgrid capability curve is much different from individual DERs; first the shape is not a circle or half circle as is common in DERs; second it has a negative part as well which is resulted from battery charging. However similar to individual DERs' capability curves, once microgrid's capability curve is

obtained, a closed form mathematical model can be fitted into the curve to be used for ancillary service studies.

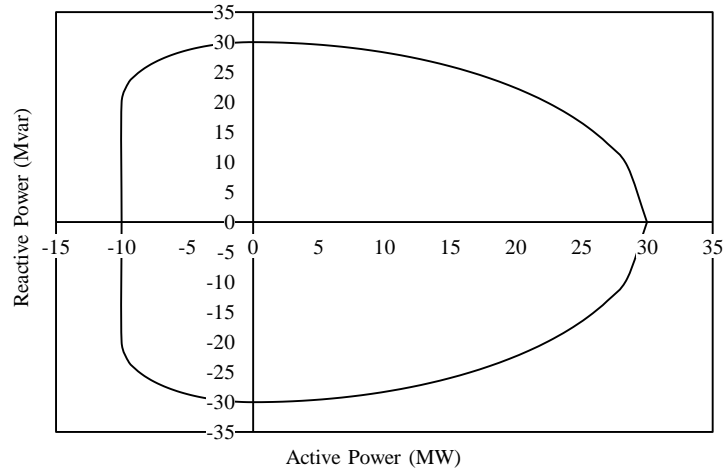


Figure 3.3. Capability curve of microgrid for Case1.

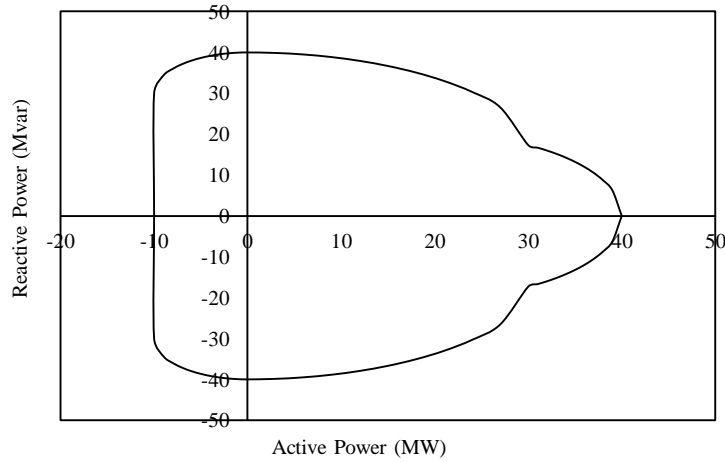


Figure 3.4. Capability curve of microgrid for Case 2.

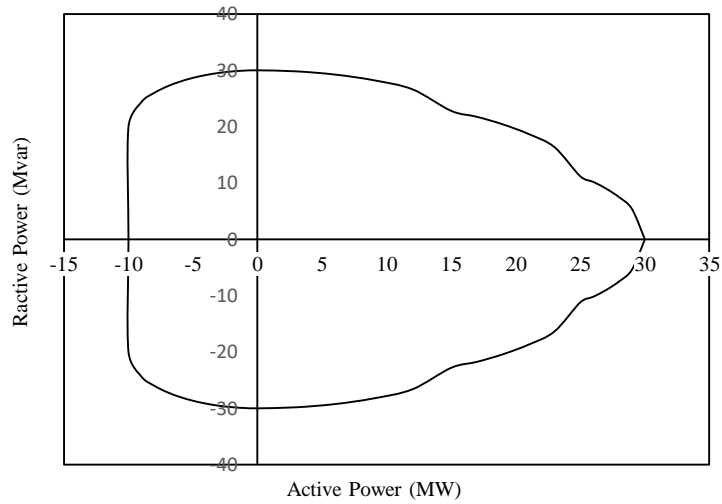


Figure 3.5 Capability curve of microgrid for Case 3.

3.4 Discussion

Microgrids can be utilized as ancillary service providers in the distribution grid, besides all their other benefits. Accordingly, capability curve of microgrid plays a key role in participating in ancillary service market. This chapter developed an optimization-based model to find the capability curve of microgrid as a single unit. The numerical analyses were carried out in various cases and the obtained results showed that the capability curve of microgrid depends on the capacity of its DERs. The shape of capability curve would be significantly changed when the DERs have different capacities and sizes. This capability curve would be used during the microgrid power sharing at the load buses under its reactive power constrains.

CHAPTER FOUR: MICROGRID EFFECT ON OPERATION COST

As discussed in the previous chapter, a microgrid consists of interconnected distributed generators and loads that can work in a coordinated fashion in grid-connected and island modes. Microgrids offer several benefits to customers and the grid, including but not limited to, improving reliability and resilience, improving energy efficiency and reducing transmission and distribution costs. Microgrids can further be utilized as a source of ancillary services at the distribution grid.

The objective of this chapter is to find the role that microgrids can play in offering reactive power, as a vital ancillary service, to the grid. This is performed by leveraging the microgrid capability curve, which shows the relationship between its real and reactive power generation, and accordingly investigating how much service the microgrid can provide based on respective capability limits.

4.1 Model Outline and Formulation

The capability curve of any electrical generator is defined as a boundary within which the machine can operate safely. The microgrid capability curve model is built upon the minimum and the maximum reactive power that can be produced by the microgrid based on the net real power it produces. This objective is subject to constraints associated with microgrid's energy resources, such as solar PV, battery, and the synchronous generator, as well as its local load.

The following equations (4.1)-(4.7) describe how the microgrid capability curve is obtained based on different sizes of interconnected DERs. For each real power value, there is a positive and a negative limit for the reactive power for each source of the microgrid. The total limit of the reactive power is equal to the summation of that of all sources (4.1)-(4.6), and the incremental increasing of the real power for each unit as illustrated in (4.7).

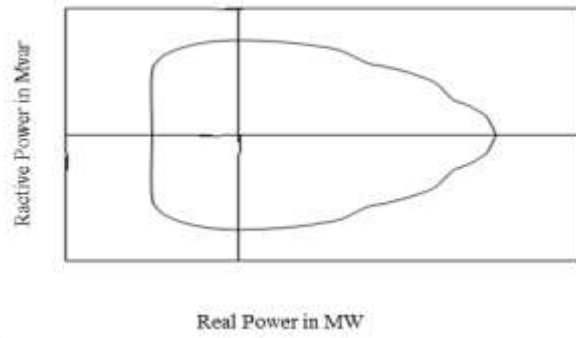


Fig.4.1 Microgrid Capability Curve

Fig. 1 shows an illustrative example of the capability curve of a microgrid that is obtained based on (4.1)-(4.7).

$$S_1 < S_2 < S_3$$

$$\text{For } P_i \leq S_1$$

$$Q_i^{max} = \sqrt{S_1^2 - P_i^2} + \sqrt{S_2^2 - P_i^2} + \sqrt{S_3^2 - P_i^2} \quad (4.1)$$

$$Q_i^{min} = -\sqrt{S_1^2 - P_i^2} - \sqrt{S_2^2 - P_i^2} - \sqrt{S_3^2 - P_i^2} \quad (4.2)$$

$$\text{For } S_1 < P_i \leq S_2$$

$$Q_i^{max} = \sqrt{S_2^2 - P_i^2} + \sqrt{S_3^2 - P_i^2} \quad (4.3)$$

$$Q_i^{min} = -\sqrt{S_2^2 - P_i^2} - \sqrt{S_3^2 - P_i^2} \quad (4.4)$$

For $S_2 < P_i \leq S_3$

$$Q_i^{max} = +\sqrt{S_3^2 - P_i^2} \quad (4.5)$$

$$Q_i^{min} = -\sqrt{S_3^2 - P_i^2} \quad (4.6)$$

$$P_{i+1} = P_i + 1 \quad (4.7)$$

The modified power flow is proposed as in (4.8)-(4.15). The objective of the proposed model is to minimize the total generation cost (4.8) which is a second order function of real power generation. The objective function is subject to load flow and power balance equations (4.9)-(4.15).

$$\min \sum_t (a_p P_{it}^2 + b_p P_{it} + c_p) \quad \forall i \in G \quad (4.8)$$

$$PL_{mnt} = g_{mn} V_{mt}^2 - V_{mt} V_{nt} (g_{mn} \cos(\theta_{mt} - \theta_{nt})) \\ - V_{mt} V_{nt} (b_{mn} \sin(\theta_{mt} - \theta_{nt})) \quad \forall mn \in L, \forall t \quad (4.9)$$

$$QL_{mnt} = -b_{mn} V_{mt}^2 - V_{mt} V_{nt} (b_{mn} \cos(\theta_{mt} - \theta_{nt})) \\ - V_{mt} V_{nt} (g_{mn} \sin(\theta_{mt} - \theta_{nt})) \quad \forall mn \in L, \forall t \quad (4.10)$$

$$-PL_{mn}^{max} \leq PL_{mnt} \leq PL_{mn}^{max} \quad \forall mn \in L, \forall t \quad (4.11)$$

$$-QL_{mn}^{max} \leq QL_{mnt} \leq QL_{mn}^{max} \quad \forall mn \in L, \forall t \quad (4.12)$$

$$\sum_{i \in G} P_{it} + \sum_{n \in B_m} PL_{mnt} = PD_{mt} \quad \forall m, \forall t \quad (4.13)$$

$$\sum_{i \in G} Q_{it} + \sum_{n \in B_m} QL_{mnt} = QD_{mt} + QM_{mt} \quad \forall m, \forall t \quad (4.14)$$

$$V_m^{min} \leq V_{mt} \leq V_m^{max} \quad \forall m, \forall t \quad (4.15)$$

Lines' real and reactive power flow equations are provided in (4.9) and (4.10), respectively. Equations (4.11) and (4.12) ensure that lines' real and reactive power are limited by their flow limits. The nodal real and reactive power balance equations (4.13) ensure that the sum of the power from microgrid and the power coming from the lines connected to each bus is equal to the load at that bus. In nodal reactive power balance equation (4.14), a variable is added to calculate the optimum reactive power of the microgrid installed at each bus to compensate it. Equation (4.15) represents the limit of voltage magnitude for each bus in the power system. The objective of this model is to find the system operation cost under sharing of real power at load bus under constraints of minimum and maximum reactive power that can be produced by the microgrid based on the net real power it produces on the capability curve of the microgrid.

4.2 Numerical Simulation

The proposed model is formulated in MATPOWER and applied to IEEE 57-bus standard test systems. This system consists of seven generators and fifty load buses.

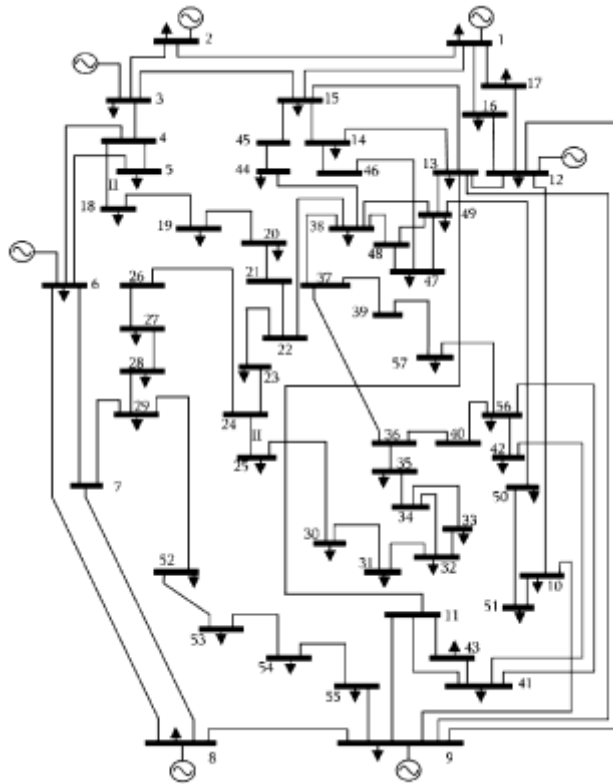


Fig.4.2. IEEE 57- bus standard system

4.2.1 Microgrid instillation at Critical Bus:

The critical bus is where the objective function is highly effected by optimal reactive power. For this test system, bus 35 is one of these critical buses. A microgrid with DG characteristics as in Table 4.1.is considered to be connected to this bus. Table 4.2 shows the change in the system operation cost when the microgrid is grid-connected and should supply a local load of 6 MW/3 MVAR. Table 4.3 shows similar case but ignores the microgrid capability curve to find out the optimal unconstrained reactive power

Table.4.1 Microgrid Interconnected Sizes

Synchronous Generator (MVA)	Photovoltaic Cell (MVA)	Storage Battery (MVA)
2	2	2

Table.4.2. Total system operation cost under different scenarios – considering microgrid capability curve

Real power demand of the Microgrid	Real power from the grid	Microgrid reactive power limit	System operation cost (at marginal cost of \$27.7/MWh)	System operation cost (at marginal cost of \$39.1/MWh)	System operation cost (at marginal cost of \$65.6/MWh)
0	6	6	41732	41732	41732
1	5	5.9	41708	41719	41746
2	4	5.6	41688	41711	41764
3	3	5.1	41668	41702	41782
4	2	4.47	41649	41695	41801
5	1	3.31	41630	41687	41820
6	0	0	41612	41680	41839

TABLE.4.3. Total system operation cost under different scenarios – ignoring microgrid capability curve

Real power demand of the Microgrid	Real power from the grid	Optimal Reactive Power	System operation cost (at marginal cost of \$27.7/MWh)	System operation cost (at marginal cost of \$39.1/MWh)	System operation cost (at marginal cost of \$65.6/MWh)
0	6	12.8	41722	41722	41722
1	5	12.76	41703	41714	41741
2	4	12.72	41684	41707	41760
3	3	12.68	41665	41699	41779
4	2	12.65	41646	41692	41798
5	1	12.62	41628	41685	41817
6	0	12.59	41609	41678	41837

As the microgrid gradually introduced through the grid at bus 35, there is a large observable change in the system operation cost especially when the microgrid was fully introduced. When microgrid offers a small marginal cost, such as in \$27.7/Mwh or \$39.1/Mwh as shown in Tables 4.2 and 4.3, it could be beneficial in reducing system operation cost. However, this is not the case when the microgrid marginal cost is higher as at \$65.6/Mwh. On the other hand, during gradual introducing of the microgrid, the difference in microgrid operation cost under capability curve limit and under optimum reactive power is noticed. That is like when the microgrid is fully introduced at \$ 27.7 as a marginal cost, the system operation cost was \$ 441612 under microgrid reactive power limits, while that was \$ 441609 under microgrid with optimal reactive power operation at 0.007% decreasing percent. This seems as a small percentage, but in practical system, the operation cost is considered extremely high (in range of millions of dollars daily), this reduction can lead to significant savings.

4.2.2 Microgrid Instillation at Noncritical Bus

A microgrid was deployed at bus 38 which is a noncritical bus. The interconnected generators of micro synchronous generator and renewable sources are equal in sizes with 5 MVA as illustrated in Table 4.4 Tables 4.5 and 4.6 illustrate the change in operation cost under sharing of real power at different points under reactive power constraint of microgrid capability curve and under optimal reactive power, respectively.

Table 4.4 Microgrid Interconnected Sizes

Synchronous Generator (MVA)	Photovoltaic Cell (MVA)	Storage Battery (MVA)
5	5	5

Table.4.5. Total system operation cost under different scenarios – considering microgrid capability curve

Real power demand of the Microgrid	Real power from the grid	Microgrid reactive power limit	System operation cost (at marginal cost of \$27.7/MWh)	System operation cost (at marginal cost of \$39.1/MWh)	System operation cost (at marginal cost of \$65.6/MWh)
0	14	15	41727	41727	41727
1	13	14.96	41709	41721	41747
2	12	14.86	41692	41715	41768
3	11	14.69	41675	41709	41788
4	10	14.45	41657	41703	41809
5	9	14.14	41640	41697	41830
6	8	13.77	41623	41692	41850
7	7	13.27	41606	41686	41871
8	6	12.7	41589	41680	41892
9	5	12	41572	41675	41913
10	4	11.18	41555	41669	41934
11	3	10.19	41539	41664	41955
12	2	9	41522	41659	41977
13	1	7.5	41505	41653	41998
14	0	5.43	41488	41648	42019

Table.4.6 Total system operation cost under different scenarios – ignoring microgrid capability curve

Real power demand of the Microgrid	Real power from the grid	Optimal Reactive Power	System operation cost (at marginal cost of \$27.7/MWh)	System operation cost (at marginal cost of \$39.1/MWh)	System operation cost (at marginal cost of \$65.6/MWh)
0	14	17.50	41726	41726	41726
1	13	17.49	41709	41720	41746
2	12	17.45	41691	41714	41767
3	11	17.43	41674	41709	41788
4	10	17.41	41657	41703	41809
5	9	17.39	41640	41697	41830
6	8	17.36	41623	41691	41850
7	7	17.34	41606	41686	41871
8	6	17.32	41589	41680	41892
9	5	17.30	41572	41675	41914
10	4	17.29	41555	41669	41935
11	3	17.27	41539	41664	41956
12	2	17.25	41522	41659	41977

13	1	17.24	41505	41653	41998
14	0	17.22	41488	41648	42019

In bus 38, where the effect of the optimal reactive power on the system operation cost Compared to that under the microgrid limits could be seen. Based on Optimal Reactive power effect on the objective function at Case IEEE 57 The bus 35 is critical bus, while bus 38 isn't critical, but based on Table 4.2,4.3,4.5, and 4.6, microgrid instillation at these buses makes bus 38 more critical than bus 35. The microgrid instillation reorders the critical buses. The following Table 4.7 the new critical buses based on the microgrid instillation for Case IEE57 beside the buses due to optimal reactive power operation only.

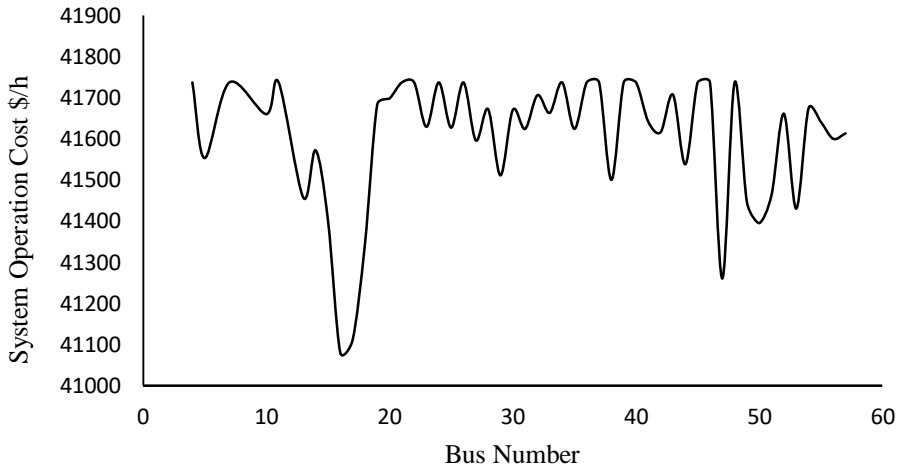


Fig. 4.3. Microgrid Effect on Object Function at Load Buses for Case IEEE57

The Microgrid instillation at P- Q buses of Case IEEE 57 has larger effect than that of optimal reactive power operation. The bus number 16 on microgrid instillation decreased

the basic objective 41738 \$/h to 41080 \$/h by -1.57 %, while bus number 36 decreased the basic objective function to 41721.65 \$/h by -0.04%.

Table.4.7 The System Operation Cost Comparison between optimal reactive power and Microgrid

Microgrid Critical Buses		Optimal Reactive Power Critical Buses	
Bus Number	System Operation Cost \$/h	Bus Number	System Operation Cost \$/h
16	41080	36	41721.65
17	41110	35	41722.27
47	41260	40	41722.84
18	41343	37	41723.59
50	41395	34	41723.68
15	41403	32	41725.21
53	41430	39	41725.71

4.3 Conclusion

Introducing microgrid in a power system at load buses results in observable reduction in the system operation cost more than that of optimal reactive power operation only, as operating cost of microgrid is very low compared to large scale electrical synchronous generators. In addition to that, due to losses reduction and due to closeness between generation and consumption. As the operation cost of the microgrid stays low, using a microgrid as a source of real power and reactive power is reasonable, but as microgrid operation cost increases, at certain value, introducing the microgrid doesn't provide expected benefit. When the microgrid installed at load buses individually, the critical buses that released are different from that when the grid operated under the optimal reactive power only. In addition, the effect of microgrid operation under its capability curve constrains is different in small percent when that is compared to its operation under presence of optimal reactive power. Even this is small, it has a valuable benefit at large power system where the operation goes high.

CHAPTER FIVE: CONCLUSION AND FUTURE WORK

Reactive power is one of the most important ancillary services to ensure a stability and reliable delivery of electricity in power systems. It further contributes to the improvement of the quality of the service. In this dissertation, another potential and less-investigated benefit of reactive power was discussed, i.e., the impact in providing economic benefits by reducing the system operation cost. Reactive power readjustment at load buses can reduce system operation cost while keeping bus voltages at acceptable range. Optimal reactive power at each load bus has a different degree of impact on system operation cost compared to other buses, which is negligible in some cases and considerable in some other. Either way, even the smallest improvements could translate to millions of dollars in savings for system operators and end-use customers given the significantly larger size of practical systems. In this dissertation, it was studied how microgrids can provide this nodal reactive power to further support grid economics. The practical limitations, enforced by the capability curve of each individual DER within the microgrid, were further modeled and considered. The results of simulations on standard test systems proved that microgrid can certainly be beneficial in supporting the grid economics by offering reactive power. Considering microgrid for providing additional ancillary services, such as reserve, ramping, and flexibility, can be considered as a next step. In addition, the identification of

system-wide coordinated optimal reactive power can be a potential next step which can be achieved by extending the proposed models in this dissertation.

REFERENCES

- [1] N. Jelani, M. Molinas and S. Bolognani, "Reactive Power Ancillary Service by Constant Power Loads in Distributed AC Systems" (IEEE Transactions on Power Delivery, volume 28, number 2, April 2013, pages 920-927).
- [2] Q. Liu, M. Cao and D. Wang, "The analysis of the reactive power ancillary service of regional grid" (2011 International Conference on Electronics, Communications and Control (ICECC), Ningbo, 2011, pages 2332-2335).
- [3] A. Ellis, R. Nelson, E. Engeln, R. Walling, J. MacDowell, L. Casey, and E. Seymour, "Reactive power performance requirements for wind and solar plants" (IEEE Power and Energy Society General Meeting, San Diego, CA, July 2012, pages 1-8).
- [4] A. Rabiee and M. Parniani, "Optimal reactive power dispatch using the concept of dynamic VAR source value" (IEEE Power & Energy Society General Meeting, Calgary, AB, July 2009, pages 1-5).
- [5] W. Qin, P. Wang, X. Han and X. Du, "Reactive Power Aspects in Reliability Assessment of Power Systems" (IEEE Transactions on Power Systems, volume 26, February 2011, pages 85-92).
- [6] V. Tejwani, B. Suthar, and D. Prajapati, "Integration of microgrid with utility grid for sharing real and reactive power" (International Conference on Computer, Communication and Control (IC4), Indore, September 2015, pages 1-5).

- [7] Y. Liu, Y. Wang, M. Li, N. Xu, W. Wang, N. Wang, H. Wang, and J. Wu, "Improvement of reactive power dynamic response for virtual synchronous generator" (IEEE 8th International Power Electronics and Motion Control Conference (IPEMC-ECCE Asia), Hefei, May 2016, pages 2010-2014).
- [8] J. Y. Choi, S-H. Rim and J-K. Park, "Optimal real time pricing of real and reactive powers" (IEEE Transactions on Power Systems, volume 13, number 4, November 1998, pages 1226-1231).
- [9] F. Alsokhiry and K. Lo, "Provision of reactive power support ancillary services from distributed generation based on renewable energy" (International Conference on Renewable Energy Research and Applications (ICRERA), Madrid, October 2013, pages 1018-1023).
- [10] J. Zhong and K. Bhattacharya, "Toward a competitive market for reactive power," (IEEE Transactions on Power Systems, volume 17, number 4, November 2002, pages 1206-1215).
- [11] G. Vaidya, N. Gopalakrishnan, and Y. Nerkar, "Cost based reactive power pricing structure in restructured environment" (Joint International Conference on Power System Technology, New Delhi, pages 1-8, October 2008).
- [12] M. Ippolito, F. Massaro, G. Pecoraro, E. Sanseverino, "Economical evaluations of reactive power supply as an ancillary service offered by Distributors" (IEEE PES General Meeting, Montreal, Canada, June 2006, pages 1-5).

- [13] X. J. Lin, C. W. Yu and C. Y. Chung, "Pricing of reactive support ancillary services" (IEE Proceedings - Generation, Transmission and Distribution, volume 152, number 5, September 2005, pages 616-622).
- [14] S. Surender Reddy, A.R. Abhyankar, P.R. Bijwe, "Reactive power price clearing using multi-objective optimization" (Energy, volume 36, number 5, March 2011, pages 3579-3589).
- [15] J. Zhong, E. Nobile, A. Bose and K. Bhattacharya, "Localized reactive power markets using the concept of voltage control areas" (IEEE Transactions on Power Systems, volume 19, number 3, Aug. 2004, pages 1555-1561).
- [16] J. Zhong and K. Bhattacharya, "Toward a competitive market for reactive power," (IEEE Transactions on Power Systems, volume 17, number 4, November 2002, pages 1206-1215).
- [17] M. Guarnieri, A. Bovo, A. Giovannelli and P. Mattavelli, "A real multitechnology microgrid in Venice: A design review" (IEEE Industrial Electronics Magazine, volume 12, number 3, September 2018, pages 19-31).
- [18] S. Parhizi, H. Lotfi, A. Khodaei and S. Bahramirad, "State of the art in research on microgrids: A review" (IEEE Access, volume 3, June 2015, pages 890-925).
- [19] Q. Li, Z. Xu, and L. Yang, "Recent advancements on the development of microgrids" (Journal Modern Power System Clean Energy, volume 2, number 3, September 2014, pages 206–211).

- [20] A.G. Madureira, J.A. Peças Lopes, "Ancillary services market framework for voltage control in distribution networks with microgrids" (Electric Power Systems Research, volume 86, May 2012, pages 1-7).
- [21] C. Yuen, A. Oudalov, "The feasibility and profitability of ancillary services provision from multi-microgrids" (IEEE Lausanne Power Tech, Lausanne, July 2007, pages 598-603).
- [22] A. Majzoobi, A. Khodaei, "Application of microgrids in providing ancillary services to the utility grid" (Energy, volume 123, March 2017, pages 555-563).
- [23] A. Rabiee, M. Parniani, "Optimal reactive power dispatch using the concept of dynamic VAR source value" (IEEE Power & Energy Society General Meeting, Calgary, AB, July 2009, pages 1-5).
- [24] Q. Wang, B. Wang, W. Xu and J. Xu, "Research on STATCOM for reactive power flow control and voltage stability in microgrid" (2018 13th IEEE Conference on Industrial Electronics and Applications (ICIEA), Wuhan, 2018, pages 2474-2479).
- [25] M.T.L. Gayatri, Alivelu.M. Parimi, A.V. Pavan Kumar, "A review of reactive power compensation techniques in microgrids" (Renewable and Sustainable Energy Reviews, volume 81, January 2018, pages 1030-1036).
- [26] M. M. Adibi and D. P. Milanicz, "Reactive capability limitation of synchronous machines" (IEEE Transactions on Power Systems, volume 9, number 1, February 1994, pages 29-40).

- [27] R. Albarracín, M. Alonso "Photovoltaic reactive power limits" (12th International Conference on Environment and Electrical Engineering, Wroclaw, Poland, May 2013, pages 13-18).
- [28] F. Delfino, G. B. Denegri, M. Invernizzi, R. Procopio and G. Ronda "A P-Q capability chart approach to characterize grid connected PV-units" (2009 CIGRE/IEEE PES Joint Symposium Integration of Wide-Scale Renewable Resources Into the Power Delivery System, Calgary, AB, 2009, pages 1-8).
- [29] H. Li, Y. Xu, S. Adhikari, D. T. Rizy, F. Li and P. Irmingier, "Real and reactive power control of a three-phase single-stage PV system and PV voltage stability" (2012 IEEE Power and Energy Society General Meeting, San Diego, CA, 2012, pages 1-8).
- [30] T. Hosseinimehr, A. Ghosh, F. Shahnia, "Cooperative control of battery energy storage systems in microgrids" (International Journal of Electrical Power & Energy Systems, volume 87, May 2017, pages 109-120).
- [31] C. A. Hill, M. C. Such, D. Chen, J. Gonzalez and W. M. Grady, "Battery energy storage for enabling integration of distributed solar power generation" (IEEE Transactions on Smart Grid, volume 3, number 2, June 2012, pages 850-857).
- [32] O. Adeyemo, P. Idowu, A. Asrari and J. Khazaei, "Reactive power control for multiple batteries connected in parallel using modified power factor method" (2018 North American Power
- [33] F. Alsokhiry and K. Lo, "Provision of reactive power support ancillary services from distributed generation based on renewable energy," In International

- Conference on Renewable Energy Research and Applications (ICRERA), pp. 1018-1023, 2013.
- [34] Q. Liu, M. Cao, D. Wang. "The analyses of the reactive power as Ancillary services of Regional Grid", IEEE transaction pp2332.
- [35] Y. Liu, Y. Wang, M. Li, N. Xu, W..Wang, N. Wang, H. Wang, and J. Wu, "Improvement of reactive power dynamic response for virtual synchronous generator," In 2016 IEEE 8th International Power Electronics and Motion Control Conference (IPEMC-ECCE Asia), pp. 2010-2014, 2016.
- [36] W. Qin, P. Wang, X. Han, and X. Du, "Reactive power aspects in reliability assessment of power systems," IEEE Transactions on Power Systems, pp. 85-92, 2011.
- [37] M. Omar and G. Scarcella, "Unbalanced and reactive power compensation for grid friendly microgrids," 3rd Renewable Power Generation Conference, Naples, Italy, 2014.
- [38] R. Pontes, J. Filho, and P. La Gatta, "A full Newton approach to consider reactive power generation limits in power flow problem using sigmoid switches," 2018 Simposio Brasileiro de Sistemas Eletricos (SBSE), 2018
- [39] J. Qiao, Y. Min, and Z. Lu, "Optimal reactive power flow in wind generation integrated power system," In 2006 International Conference on Power System Technology, pp. 1-5, 2006.

- [40] M. Hunyár and K. Veszprémi, “Reactive power control of wind turbines,” In 16th International Power Electronics and Motion Control Conference and Exposition, pp. 348-352, 2014.
- [41] B. Igor, and P. Evgen, “Approach of reactive power pricing for ancillary service of voltage control in Ukraine,” In 2014 IEEE International Conference on Intelligent Energy and Power Systems (IEPS), pp. 145-148, 2014.
- [42] V. Tejwani, B. Suthar, and D. Prajapati, “Integration of microgrid with utility grid for sharing real and reactive power,” In 2015 International Conference on Computer, Communication and Control (IC4), pp. 1-5, 2015.
- [43] A. Engler and N. Soultanis, “Droop control in LV-grids,” 2005 International Conference on Future Power Systems, 2005.
- [44] S. Mohanty, S. Sen, N. Kishor, P. Ray, and V. Singh, “Harmonic compensation in distributed generation based micro-grid using droop control technique,” In 2011 5th International Power Engineering and Optimization Conference, pp. 233-237, 2011.
- [45] M. Ippolito, F. Massaro, G. Pecoraro, E. Sanseverino, “Economical evaluations of reactive power supply as an ancillary service offered by Distributors,” Proceeding of IEEE PES General Meeting, 18-22 June 2006, Montreal, Canada.
- [46] K. Umamaheswari, P. L. Somasundaram, “Pricing framework for reactive power as ancillary service,” 2014 International Conference on Electronics and Communication Systems (ICECS), 2014.

- [47] P. Ribeiro, L. Marzano, J. Soto, R. Prada, and A.Melo, "Methodology to remunerate the generation reserve and the reactive power support as ancillary services based on the benefit proportioned to the power system," In IEEE Russia Power Tech, pp. 1-7, 2005."
- [48] Z. Junfang, M. Qinguo, and D. Xinzhou, "Real-time pricing of reactive power considering value of reactive power resources," In China International Conference on Electricity Distribution, pp. 1-6, 2008.
- [49] M. Mahala, and Y. Kumar, "Active & reactive power rescheduling for congestion management using new PSO strategy," In 2016 IEEE Students' Conference on Electrical, Electronics and Computer Science (SCEECS), pp. 1-4., 2016.
- [50] A. Rabiee and M. Parniani, "Optimal reactive power dispatch using the concept of dynamic VAR source value," In 2009 IEEE Power & Energy Society General Meeting, pp. 1-5, 2009.
- [51] M. Abdelaziz, "Effect of detailed reactive power limit modeling on islanded microgrid power flow analysis," IEEE Transactions on Power Systems, no. 2, pp. 1665-1666, 2016.
- [52] M. Abdelaziz, "Effect of detailed reactive power limit modeling on islanded microgrid power flow analysis," IEEE Transactions on Power Systems, no. 2, pp. 1665-1666, 2016.
- [53] A. Gabash, and P. Li, "Active-reactive optimal power flow in distribution networks with embedded generation and battery storage," IEEE Transactions on Power Systems, no. 4, pp. 2026-2035, 2012.

- [54] Z. Machado, G. Taranto, and D. Falcao, "An optimal power flow formulation including detailed modeling of generators," In IEEE PES Power Systems Conference and Exposition, pp. 960-965, 2004.
- [55] W. Zheng-Feng, "Review on reactive pricing in power system market". Anhui Electric Power, vol.24, No. 4, PP.65-68, 2007.
- [56] . Wang, R. G. Yang, F. S. Wen, "On the Procurement and Pricing of Reactive Power Service in the Electricity Market Environment", IEEE Power Engineering Society General Meeting, Vol. 1, pp. 1120–1124, June 2004
- [57] X. Lin, C. Yu, and C. Chung, "Pricing of reactive support ancillary services," IEE Proceedings-Generation, Transmission and Distribution 152, no. 5, pp. 616-622, 2005.
- [58] F. Moschetti, S. Paoletti, and A. Vicino. "Analysis and models of electricity prices in the Italian ancillary services market," In IEEE PES Innovative Smart Grid Technologies, Europe, pp. 1-6, 2014.
- [59] J. Choi S. Rim, and J. Park, "Optimal real time pricing of real and reactive powers," IEEE Transactions on Power Systems, no. 4, pp. 1226-1231, 1998.
- [60] G. Vaidya, N. Gopalakrishnan, and Y. Nerkar. "Cost based reactive power pricing structure in restructured environment," In 2008 Joint International Conference on Power System Technology, pp. 1-8, 2008.
- [61] J. Zhong, and K. Bhattacharya, "Toward a competitive market for reactive power," IEEE Transactions on Power Systems, no. 4 pp. 1206-1215, 2002.

- [62] H. Moreno, S. Plumel, and P. Bastard, "Assessing the value of reactive power service using OPF of reactive power," In 2005 IEEE Russia Power Tech, pp. 1-6, 2005.
- [63] A. Rabiee, H. Ali, and N. Amjady, "Reactive power pricing problems and a proposal for a competitive market," IEEE Power and Energy Magazine, January and February 2009
- [64] A. Ellis, R. Nelson, E. Engeln, R. Walling, J. MacDowell, L. Casey, and E. Seymour, "Reactive power performance requirements for wind and solar plants," In 2012 IEEE Power and Energy Society General Meeting, pp. 1-8, 2012.
- [65] A. Cabrera-Tobar, E. Bullich-Massagué, M. Aragüés-Peñalba, O. Gomis-Bellmunt, "Topologies for large scale photovoltaic power plants" (Renewable and Sustainable Energy Reviews, volume 59, June 2016, pages 309-319).
- [66] A. Cabrera-Tobar, E. Bullich-Massagué, M. Aragüés-Peñalba, O. Gomis-Bellmunt, "Reactive power capability analysis of a photovoltaic generator for large scale power plants" (5th IET International Conference on Renewable Power Generation (RPG), London, 2016, pages 1-6).
- [67] J. Huang, M. Liu, J. Zhang, W. Dong, and Z. Chen "Analysis and field test on reactive capability of photovoltaic power plants based on clusters of inverters" (Journal of Modern Power Systems and Clean Energy, volume 5, number 2, March 2017, pages 283-289).
- [68] A. Khodaei, "Microgrid optimal scheduling with multi-period islanding constraints". IEEE Transactions on Power Systems, 29(3), pp.1383-139

APPENDIX A: OPTIMAL REACTIVE POWER CODES

.The matpower codes to calculate the objective function at optimal reactive power at each load bus
individually of case IEEE 57

```
define_constants;
foptimal = fopen('f.csv','w');
B= [4 5 7 10 11 13 14 15 16 17 18 19 20 21 22 23 24 25 26 27 28 29 30 31 32 33 34 35 36 37 38 39
40 41 42 43 44 45 46 47 48 49 50 51 52 53 54 55 56 57];
j=8;
for I=1:50
    A=B(i);
    P=200;
    mpc=loadcase('case57c');
    ng = size(mpc.gen, 1) + 1;
    mpc.bus (A,BUS_TYPE)= 2;
    mpc.gencost(j,MODEL)=2;
    mpc.gen(ng, GEN_BUS:PMIN) = [A 0 0 P -P 1 100 1 0 0];
    mpc = runopf(mpc);
    x=mpc.f;
    fprintf(foptimal,'%f%f\n',A,x);
    j = j+1;
end
fclose(foptimal);
type('f.csv');
display (foptimal)
```

Games Codes for Microgrid Capability Curve Calculation

```
set t /1*60/;
set tmp1 /1*11/;
set tmp2 /1*6/;
positive variables Sg, Ss, Sv;
variable f;
variables Qg, Qv, Ps, Qs;
Positive variables Pg, Pv;
variable Ps Energy storage power;
Parameter v;
positive variable E internal voltage of generator;
variable I generator current;
*variable Es(t) energy of DES;
v=1;
variable delta;
scalar x /0.002/;
parameter unit(tmp1)
/1    0
2    20
3    20
```

```

/;parameters Pgmin, Pgmax,Sgmax;
Pgmin=unit('1');
Pgmax=unit('2');
Sgmax=unit('3');
parameter BES(tmp2)
/1    0
2    10
3    10/
parameters Psmín,Psmax,Ssmáx;
Psmín=BES('1');
Psmax=BES('2');
Ssmáx=BES('3');
parameter PD    Active power Load at time t (MW);
PD=-20;
variable QD;
parameters
fn(t)
En(t)
deltan(t)
Pgn(t)
Psn(t)
Pvn(t)
Qgn(t)
Qsn(t)
Qvn(t)
QDn(t)
Sgn(t)
Ssn(t)
Svn(t)
PDn(t)
;
equations

con2
con3
con4
con5, con6, con7
con8, con9, con10
con11
con12
con13
con14
con15
con16
con17
obj f =e= QD;
con2. power(Sg,2) =e= power(Qg,2)+power(Pg,2);
con3 Pg +Ps + Pv =e= PD;
con4 Qg + Qs+ Qv =e= QD;
con5 Pg =l= Pgmax;
con6. Pg =g= Pgmin;
con7. Sg =l= Sgmax;

```



```

con8 power(E,2) =e= power(I*x,2)+power(v,2);
con9. Pg =e= v*E*sin(delta)/x;
con10. Qg =e= v*E*cos(delta)/x-E*E/x;
*Energy Storage Constraints
con11. Ps =l= Psmax;
con12. Ps =g= -Psmax;
con13. power(Ss,2) =e= power(Qs,2) + power(Ps,2);
con14. Ss =l= Ssmax;
*PV constraints
con15. Pv =l= 0;
con16. power(Sv,2) =e= power(Qv,2)+power(Pv,2);
con17. Sv =l= 0;
model sample Problem /all/;
*sample Problem.Optcr =0;
option threads=32;
loop(t,
solve sample Problem using MINLP minimizing f;
fn(t) = f.l;
En(t)=E.l;
deltan(t)=delta.l;
Pgn(t)=Pg.l;
Psn(t)=Ps.l;
Pvn(t)=Pv.l;
Qgn(t)=Qg.l;
Qsn(t)=Qs.l;
Qvn(t)=Qv.l;
QDn(t)=QD.l;
Sgn(t)=Sg.l;
Ssn(t)=Ss.l;
Svn(t)=Sv.l;
PDn(t)=PD;
PD=PD+1.5;
);
display fn, En, deltan
      Pgn, Psn, Pvn, PDn
      Qgn, Qsn, Qvn, QDn
      Sgn, Ssn, Svn ;
*file results/results- Sarhan.dat/ ;
*-----Results
*put results;
*Put 'Results'/;
*'/Pg:'/;
*loop(t, put acd.tl, @ 12, b.tl, @ 24, h.tl, @ 36, Pacd.l(acd,b,h):8:4 /);

```

```

Microgrid Optimal Reactive Power Matpower codes define_constants;
Foptimal = fopen ('f.csv', 'w');
B= [4 5 7 10 11 13 14 15 16 17 18 19 20 21 22 23 24 25 26 27 28 29 30 31 32 33 34 35 36 37 38 39
40 41 42 43 44 45 46 47 48 49 50 51 52 53 54 55 56 57];
j =8;
for I =1:50
    for k= 1:7
        A=B(i);
        P=200;
        mpc=loadcase('case57c');
        ng = size(mpc.gen, 1) + 1;
        mpc.bus (A,BUS_TYPE)= 2;
        mpc.gencost(j,MODEL)=2;
        mpc.gen(ng, GEN_BUS:PMIN) = [A 0 0 P -P 1 100 1 0 0];
        mpc = runopf(mpc);
        x=mpc.f;
        fprintf(foptimal, '%f %f\n',A,x);
        mpc.bus(35,PD)=k ;
        z= x + 27.7,
        end
    end
end
fclose(foptimal);
type('f.csv');
display (foptimal)

```

APPENDIX B: LIST OF PUBLICATIONS

- [1] Sarhan H. Alwan Hasan, Abdulmunim Guwaeder “Wind Energy Assessment of the Zawiya Region, in Northwest Libya “Energy and Power Engineering, 2017, 9, 325-331
- [2] Abdulmunim Guwaeder, Hasan Sarhan, Ibrahim Aldaouab “A study of the penetration of photovoltaic generation into the Libyan power system” 2107 IEEE Energy and Sustainability Conference (IESC), International Farmingdale, NY, USA .
- [3] S. HASAN, A. MAJZOABI, A. KHODAEI “Optimum Reactive Power Calculation for Reducing Power System Operation Cost “CIGRE US National Committee 2019 Grid of the Future Symposium, [http : //www.cigre.org](http://www.cigre.org).
- [4] S. HASAN, A. MAJZOABI, A. KHODAEI “An Optimization-based Method in Determining the Capability Curve of a Microgrid” CIGRE US National Committee 2019 Grid of the Future Symposium, [http: //www.cigre.org](http://www.cigre.org).